Metrol. Meas. Syst., Vol. 31 (2024), No. 2
DOI: 10.24425/mms.2024.148547

METROLOGY AND MEASUREMENT SYSTEMS
Index 330930, ISSN 0860-8229
www.metrology.wat.edu.pl

UNCERTAINTY ANALYSIS FOR THE FREE SPACE THREE-DIMENSIONAL MEASUREMENT OF ELECTROMAGNETIC PULSE

Yuewu Shi, Wei Wang, Xin Nie, Jianguo Miao, Wei Chen

National Key Laboratory of Intense Pulsed Radiation Simulation and Effect, Northwest Institute of Nuclear Technology, Xi'an, 710024, China (✉ *shiyuewu@nint.ac.cn*)

Abstract

Because the polarization direction is unknown in free-space three-dimensional (3D) electromagnetic pulse (EMP) measurement, the components in three directions are usually measured first, and then the total vector is calculated. The waveform (magnitude) and polarization direction define the 3D process. Because of the uncertainty produced in component measurement, there is also uncertainty in the calculated 3D process. This paper investigates the propagation of uncertainty during the total vector calculation process. The magnitude and polarization angle uncertainty propagation formulas are derived through analysis. The results show that the uncertainty of the calculated magnitude is less than the maximal measurement uncertainty of the three components, and the uncertainty of the polarization angle is less than sqrt(2) times the maximal uncertainty of the three components divided by the magnitude of the measured field. Finally, a Monte-Carlo (MC) simulation is run to validate the results of the analysis. The simulation results agree well with the analysis results.

Keywords: uncertainty, three-dimensional, measurement, electromagnetic pulse.

1. Introduction

Measurement is an important method for obtaining the parameters of the *electromagnetic pulse* (EMP) in the field of electromagnetic compatibility and high-power electromagnetism. In practice, measuring free space *three-dimensional* (3D) EMP is of great interest. The magnitude and polarization in spherical coordinates or three components in rectangular coordinates are commonly used to characterize the 3D EMP. The two groups of parameters characterized by spherical coordinates and rectangular coordinates can be converted to each other. In practice, the EMP is measured by first measuring the *one-dimensional* (1D) components of three orthogonal directions, and then calculating the magnitude and polarization direction of the 3D process. The components can be measured simultaneously by different kinds of 3D detectors, such as the 3D pulsed electrical detectors [1-3] and the 3D optical passive electric field sensors [4-6].

In measurement, we are concerned not only with the measured results but also with measurement uncertainty. In fact, the component measurement method is equivalent to measuring the components simultaneously with three independent 1D detectors with measurement uncertainty. The measurement uncertainty of each independent component is commonly evaluated using the *Guide to the Expression of Uncertainty in Measurement* (GUM) [7] or the *Monte-Carlo method* (MCM) [8, 9]. More specifically, there have been numerous studies on the uncertainty evaluation focusing on the sensor-based measurement of EMP [10-13]. Regarding the engineering application, the measurement uncertainty of the EMP measurement can be roughly divided into three sources: the uncertainty of the measurement system itself, the uncertainty introduced in the calibration [14], and the uncertainty introduced

Article history: received August 8, 2023; revised January 6, 2024; accepted January 17, 2024; available online February 28, 2024.

by the measurement implementation [15]. We prefer to use the GUM method to estimate the measurement due to the constantly changing state and environment involved in measurement, taking engineering applications into consideration. In most cases, Type A uncertainty statistics are used to determine the measurement system's uncertainty itself. The uncertainty in the calibration and measurement process is usually determined by the GUM method which combines Type A uncertainty with Type B uncertainty. For the calibration of pulsed electric field sensors based on the standard field method, the calibration uncertainty can be obtained through hybrid methods such as calculation and analysis [16, 17]. The uncertainty propagation process for the fitting method of calibration data during the fitting can be estimated as well [18]. Factors such as measurement position polarization direction mismatch are taken into account for the measurement procedure, and a relative reasonable analysis result can also be obtained [19]. The measurement uncertainty of a 1D measurement system can thus be obtained based on the existing methods and processes.

However, a single 1D component's uncertainty can't directly represent the uncertainty of the magnitude and polarization direction of the 3D process. The uncertainties of the components are related to the uncertainties of the calculated magnitude and polarization directions. It is necessary to study the uncertainty propagation in the calculation process and obtain an estimation formula corresponding to the uncertainties of components in order to evaluate the 3D EMP calculation. This paper investigates the uncertainty propagation of the 3D EMP during the calculation process based on the measured 1D components. Section II describes the uncertainty modelling; Section III analyzes the uncertainty of the magnitude and polarization direction by the GUM method; Section IV verifies the analysis conclusion by MCM method; and Section V summarises this article.

2. Uncertainty modelling

An arbitrary electromagnetic process under measurement can be divided into three orthogonal components. The electric field under measurement is defined as (1). The results apply to the magnetic measurements.

$$\boldsymbol{E} = \left[E_1, E_2, E_3 \right] , \tag{1}$$

where $\boldsymbol{E}$ denotes the process under measurement, and E_1, E_2 and E_3 denote the three orthogonal components respectively.

It should be noted that E_1, E_2, and E_3 are all time-dependent parameters: $E_1(t)$, $E_2(t)$, and $E_3(t)$. As the measurement results are represented by time discrete data, we usually calculate the measurement results at different discrete times and then form the waveform of the 3D EMP based on the discrete values. As a result, the measured electromagnetic transient can be reduced to a vector for a fixed time instant t_0. The uncertainties of the three components obtained through measurement can then be represented by three values. All of the parameters used in this paper are assumed at a fixed time t_0, and the conclusions are valid at any time t.

In the measurement, the components are measured by a 3D probe, which can respond to the electromagnetic process in three different directions at the same time. Obviously, measurement uncertainty existed for each measured component. Similarly, for a fixed time t_0, the measured results can be described as (2).

$$\boldsymbol{E}_{\mathrm{m}} = \left[E_{\mathrm{m1}}, E_{\mathrm{m2}}, E_{\mathrm{m3}} \right] , \tag{2}$$

where $\boldsymbol{E}_{\mathrm{m}}$ denotes the measured process, E_{m1}, E_{m2} and E_{m3} denote the measured components, respectively.

Considering the measurement uncertainty in every component, describe the measured results as (3).

$$\boldsymbol{E}_{\mathrm{m}} = \boldsymbol{E} + \boldsymbol{\delta}, \tag{3}$$

$$\boldsymbol{\delta} = \ \delta_1, \delta_2, \delta_3 \ , \tag{4}$$

where δ_1, δ_2 and δ_3 denote the measuring errors of the components E_1, E_2 and E_3 respectively.

For a function $Y= f(X_1, X_2,\ldots X_{\mathrm{n}})$, y is the evaluated value of Y, x_1,x_2,... x_{n} is the evaluated value of X_1, X_2,..., X_{n}, and all the components are uncorrelated. The combined standard uncertainty of measurement is given by the equation of guide 10.b [20].

$$u(y) = \sqrt{\sum_{i=1}^{n} \left(\frac{\partial}{\partial x_i} f\right)^2 u^2 \ x_i} \ . \tag{5}$$

Notice that the field E_1, E_2, E_3 is the true value of the three components that the uncertainties should be 0, the uncertainties of components E_{m1}, E_{m2} and E_{m3} equal the uncertainties of measuring errors δ_1, δ_2 and δ_3 respectively based on (3) and (4). Define the uncertainties of components E_{m1}, E_{m2} and E_{m3} as u_1, u_2 and u_3, as shown in (6), which can be evaluated before measurement.

$$u_i = u \ E_{\mathrm{m}i} \ = u \ \delta_i \ , i = 1,2,3 \tag{6}$$

Based on the definition of uncertainty, the uncertainties can be calculated by (7):

$$u_i = \sqrt{\overline{\delta_i^2}}, i = 1,2,3. \tag{7}$$

The uncertainty of an EMP measurement system can be composed of Type A uncertainty and Type B uncertainty. This includes both randomness and systematic uncertainty components. The expected value can be considered as 0 for the random components. The deviation of the systematic components, however, is usually a fixed value. The uncertainty components related to the systematic deviation of an EMP measurement system mainly include the deviation of the calibration coefficient and the sensor jitter caused by temperature change. For the calibration of sensor coefficients, the calibration instruments such as oscilloscopes and attenuators in is usually traced through the metrology laboratory before calibration and eliminate their systematic errors to ensure the accuracy of the calibration devices. On the other hand, for the calibration process of the standard field method, the standard deviation generated in the calibration device is corrected according to the preliminary analysis results, and the uncertainty of the oscilloscope measurement and other processes is reduced as much as possible by the method of multiple calibration. Sensor jitter due to temperature changes is not strictly a completely systematic deviation component, but it can be approximated as a fixed deviation value compared to a very short measurement process, and similar deviations will be exhibited by similar sensors. We have also minimized it by means of sensor thermal insulation and coefficient compensation, which can technically be controlled within 1%. After considering the elimination of the above components of systemic uncertainty, it can be approximated that the expected value of the measurement uncertainty δ_i is approaching 0:

$$\delta_i = 0, i = 1,2,3. \tag{8}$$

The measured results that are characterized by rectangular coordinates commonly need to be exchanged into spherical coordinates that contain magnitude and polarization direction. The uncertainties of magnitudes can be expressed as *root-mean-square* (RMS) values as well, as shown in (9)

$$u\ |\boldsymbol{E}_{\mathrm{m}}|\ = \sqrt{\ |\boldsymbol{E}_{\mathrm{m}}| - |\boldsymbol{E}|\ ^2}, \tag{9}$$

where $|\boldsymbol{E}|$ and $|\boldsymbol{E}_{\mathrm{m}}|$ denote the magnitude of the truth-value and the calculated results based on measurement respectively.

$$|\boldsymbol{E}| = \sqrt{E_1^2 + E_2^2 + E_3^2}, \tag{10}$$

$$|\boldsymbol{E}_{\mathrm{m}}| = \sqrt{E_{m1}^2 + E_{m2}^2 + E_{m3}^2}. \tag{11}$$

Define a parameter α to denote the angle of the polarization direction between $|\boldsymbol{E}_{\mathrm{m}}|$ and $|\boldsymbol{E}|$. Considering that the value of α for a completely accurate measurement should be 0, the uncertainty of α is expressed as (12).

$$u(\alpha) = \sqrt{\overline{(\alpha - 0)^2}} = \sqrt{\overline{\alpha^2}}, \tag{12}$$

where α is calculated by (13).

$$\cos\ (\alpha) = \frac{\boldsymbol{E} \cdot \boldsymbol{E}_{\mathrm{m}}}{|\boldsymbol{E}| \cdot |\boldsymbol{E}_{\mathrm{m}}|}. \tag{13}$$

With the representation of uncertainty in magnitude and polarization, the uncertainty propagation in the calculation can be analyzed.

For the same type of measurement system, as mentioned above, there must be a correlation between any two 1D sensors due to the influence of many factors, such as the uncertainty components caused by the systematic errors. However, in the analysis below, the measurements of the three components of the sensor are considered uncorrelated. This is true based on the assumption that the uncertainty components that have a systemic impact on the measurement (*e.g.*, the systematic error of the calibration coefficients) and the factors that cause the interference of the three component measurements (*e.g.*, antenna mutual coupling) have been fully considered and deducted as much as possible. The mutual coupling and interference amongst sensors are often taken into account in the sensor design. The effect of mutual coupling between antennas is related to the frequency of the signal being measured. As the frequency of the measured electric field increases, its wavelength is comparable to that of the three-dimensional sensor, and the coupling will increase greatly. This article focuses on the measurement of electromagnetic pulses (lightning electromagnetic pulses, high-altitude electromagnetic pulses, and electrostatic discharges), which typically cover a frequency of less than 500 MHz. Generally speaking, the mutual coupling between antennas can be controlled within a small amount of field signals below 1 GHz [21]. In the case of a large impact on mutual coupling, the effect of mutual coupling between antennas will be corrected through calibration [21]. After design considerations and calibration corrections, it is possible to control the antenna mutual coupling at 2% (34 dB). If we introduce this in our formulation for the mixed derivative terms, such terms result in smaller than 2% of the magnitude of the field and can be disregarded at a first approximation. Moreover, if the systematic deviations such as the sensitivity coefficients mentioned above are fully considered and corrected before measurement, the relevant components can be controlled at a small value as well. As a result, it is possible to think of the measurement of the three components as three separate measurement operations. The three components can be considered uncorrelated parameters. The correlation coefficient between components is assumed to be zero. The uncertainty model described above applies to the magnetic measurements.

3. Uncertainties of the magnitude and polarization direction by GUM method

3.1. Uncertainty of the magnitude

According to the propagation rule of uncertainty, the uncertainty of magnitude described in (11) calculated based on the measured components can be estimated.

$$u\ |\boldsymbol{E}_{\mathrm{m}}|\ = \sqrt{\sum_{i=1}^{3}\left(\frac{\partial}{\partial E_{\mathrm{m}i}}|\boldsymbol{E}_{\mathrm{m}}|\right)^2 u_i^2}, \tag{14}$$

where

$$\frac{\partial}{\partial E_{\mathrm{m}i}}|\boldsymbol{E}_{\mathrm{m}}| = \frac{1}{2}[E_{\mathrm{m}1}^2 + E_{\mathrm{m}2}^2 + E_{\mathrm{m}2}^2]^{-\frac{1}{2}} \cdot 2E_{\mathrm{m}i} = \frac{E_{\mathrm{m}i}}{|\boldsymbol{E}_{\mathrm{m}}|}. \tag{15}$$

Therefore:

$$u\ |\boldsymbol{E}_{\mathrm{m}}|\ = \sqrt{\frac{E_{\mathrm{m}1}^2}{|\boldsymbol{E}_{\mathrm{m}}|^2}u_1^2 + \frac{E_{\mathrm{m}1}^2}{|\boldsymbol{E}_{\mathrm{m}}|^2}u_2^2 + \frac{E_{\mathrm{m}1}^2}{|\boldsymbol{E}_{\mathrm{m}}|^2}u_3^2}. \tag{16}$$

It can be seen that the uncertainty of the 3D EMP calculation results varies with the change of components (the angle between the 3D EMP direction and the reality of the 3D rectangular coordinate system in measurement). Specially, when two of the components are 0, *i.e.*, the total vector is parallel to one of the measured polarization directions, the uncertainty equals the uncertainty of this measured components, noticed that the other two components make no contribution to the measuring and calculation process. It becomes a 1D measurement problem; the estimated uncertainty based on (16) is consistent with the 1D condition.

The uncertainty of the calculated 3D EMP can be estimated based on (16). However, in actual measurement, since the accurate values of the components are unknown, the measured results of each component can be used to replace its accurate value. As the measurement uncertainty is typically small, it has little impact on the evaluated results.

To make it more convenient in the estimation of the uncertainty, an inequation is deduced based on (10) and (16), noticing that (16) contains the value of the vector under measurement, which is unknown before measurement.

$$u\ |\boldsymbol{E}_{\mathrm{m}}|\ \leq \sqrt{max\ u_1^2, u_2^2, u_3^2\ \cdot \left(\frac{E_{\mathrm{m}1}^2}{|\boldsymbol{E}_{\mathrm{m}}|^2} + \frac{E_{\mathrm{m}2}^2}{|\boldsymbol{E}_{\mathrm{m}}|^2} + \frac{E_{\mathrm{m}3}^2}{|\boldsymbol{E}_{\mathrm{m}}|^2}\right)} = max\ u_1, u_2, u_3\ . \tag{17}$$

By the same:

$$u\ |\boldsymbol{E}_{\mathrm{m}}|\ \geq \sqrt{min\ u_1, u_2, u_3\ \cdot \left(\frac{E_{\mathrm{m}1}^2}{|\boldsymbol{E}_{\mathrm{m}}|^2} + \frac{E_{\mathrm{m}2}^2}{|\boldsymbol{E}_{\mathrm{m}}|^2} + \frac{E_{\mathrm{m}3}^2}{|\boldsymbol{E}_{\mathrm{m}}|^2}\right)} = min\ u_1, u_2, u_3\ . \tag{18}$$

Write (17) and (18) into a uniform form, as shown in (23).

$$min\ u_1, u_2, u_3\ \leq u\ |\boldsymbol{E}_{\mathrm{m}}|\ \leq max\ u_1, u_2, u_3\ . \tag{19}$$

It can be seen from (19) that even though the uncertainty is correlated to the direction of the total vector compared with the established measuring coordinate, the uncertainty is always between the maximum and minimum measurement uncertainties of the three components.

The relative uncertainty should have the same boundary, as shown in (20).

$$\frac{1}{|\boldsymbol{E}_{\mathrm{m}}|}min\ u_1, u_2, u_3\ \leq u_{\mathrm{r}}\ |\boldsymbol{E}_{\mathrm{m}}|\ \leq \frac{1}{|\boldsymbol{E}_{\mathrm{m}}|}max\ u_1, u_2, u_3\ . \tag{20}$$

The uncertainties of the three components, which are known values that should be evaluated before measurement, can be used to quickly determine the uncertainty of the overall magnitude.

In engineering applications, the evaluation of uncertainty is typically not required to be extremely accurate, but it is typically important to acquire its upper bound in order to assess the measurement's accuracy. Therefore, it is acceptable to make an appropriate overestimation of uncertainty when estimating uncertainties.

Moreover, due to the detector's typical performance being identical, the three components' uncertainties will typically not vary significantly in engineering applications. Commonly, for three component detectors of the same detector, they have the same measurement principle, adopt the same development process, use the same measurement settings during measurement, and face the same uncertainty influencing factors. Therefore, the three uncertainty components can be considered approximately the same. However, computational uncertainty and cognitive uncertainty need to be considered when evaluating uncertainty, such as the uncertainty introduced by the calculation process during the sensitivity calibration and its own jitter. These are the two main factors that contribute to the difference in uncertainties. The introduction of these uncertainties results in subtle differences in measurement uncertainty in different directions. Usually, the calculation process of calibration data and the system's own stability introduce an uncertainty of about 1~2% of the total magnitude respectively. Therefore, the overall difference of 3 uncertainties can be considered to not exceed 3%. Suppose $u_1 \geq u_2 \geq u_3$, we have:

$$\frac{1}{|\boldsymbol{E}_{\mathrm{m}}|}\left(u_1 - u_3\right) \leq 3\% \,. \tag{21}$$

Based on the derivation of the upper and lower bounds shown in (24), the difference between the upper and lower bounds of this method can be controlled within 3%. In particular, (17) can be chosen to be equal when the measurement uncertainties in all three directions are the same.

3.2. Uncertainty of the polarization direction

The deviation of the polarization angle α is deduced first to evaluate the uncertainty of the polarization direction. By substituting (3) into (13), we have

$$\cos(\alpha) = \frac{\boldsymbol{E}_{\mathrm{m}} \cdot \left(\boldsymbol{E}_{\mathrm{m}} - \boldsymbol{\delta}\right)}{|\boldsymbol{E}_{\mathrm{m}}| \cdot \sqrt{\left(\boldsymbol{E}_{\mathrm{m}} - \boldsymbol{\delta}\right)^2}} \,. \tag{22}$$

Equation (22) can be expanded into the following form.

$$\begin{aligned} \cos(\alpha) &= \frac{\boldsymbol{E}_{\mathrm{m}}^2 - \boldsymbol{E}_{\mathrm{m}} \cdot \boldsymbol{\delta}}{|\boldsymbol{E}_{\mathrm{m}}| \sqrt{\boldsymbol{E}_{\mathrm{m}}^2 + \boldsymbol{\delta}^2 - 2\boldsymbol{E}_{\mathrm{m}} \cdot \boldsymbol{\delta}}} \\ &= \frac{1 - \frac{1}{\boldsymbol{E}_{\mathrm{m}}^2} \boldsymbol{E}_{\mathrm{m}} \cdot \boldsymbol{\delta}}{\sqrt{1 + \frac{1}{\boldsymbol{E}_{\mathrm{m}}^2}\left(\boldsymbol{\delta}^2 - 2\boldsymbol{E}_{\mathrm{m}} \cdot \boldsymbol{\delta}\right)}} \\ &= f_1 \cdot f_2 \end{aligned} \,, \tag{23}$$

where

$$f_1 = \left[1 + \frac{1}{\boldsymbol{E}_{\mathrm{m}}^2}\left(\boldsymbol{\delta}^2 - 2\boldsymbol{E}_{\mathrm{m}} \cdot \boldsymbol{\delta}\right)\right]^{-\frac{1}{2}}, \tag{24}$$

$$f_2 = 1 - \frac{1}{\boldsymbol{E}_{\mathrm{m}}^2}\boldsymbol{E}_{\mathrm{m}} \cdot \boldsymbol{\delta}. \tag{25}$$

As δ_i can be served as small values compared with the magnitude $|\boldsymbol{E}|$, f_1 can be obtained by expanding it to 2-order.

$$f_1 \approx 1 + \frac{\boldsymbol{E}_{\mathrm{m}} \cdot \boldsymbol{\delta}}{\boldsymbol{E}_{\mathrm{m}}^2} - \frac{\boldsymbol{\delta}^2}{2\boldsymbol{E}_{\mathrm{m}}^2} + \frac{3}{2\boldsymbol{E}_{\mathrm{m}}^4}\left(\boldsymbol{E}_{\mathrm{m}} \cdot \boldsymbol{\delta}\right)^2. \tag{26}$$

By substituting (25) and (26) into (23), and omitting the 3-order and higher-order terms, we have

$$\cos(\alpha) \approx 1 - \frac{1}{2\boldsymbol{E}_{\mathrm{m}}^2}\boldsymbol{\delta}^2 + \frac{1}{2\boldsymbol{E}_{\mathrm{m}}^4}\left(\boldsymbol{E}_{\mathrm{m}} \cdot \boldsymbol{\delta}\right)^2. \tag{27}$$

Therefore

$$\cos(\alpha) \approx 1 - \frac{1}{2\boldsymbol{E}_{\mathrm{m}}^2}\left[\sum_{i=1}^{3}\delta_i^2 - \left(\sum_{i=1}^{3}\frac{E_{\mathrm{m}i}}{|\boldsymbol{E}_{\mathrm{m}}|}\delta_i\right)^2\right]. \tag{28}$$

The cosine value of polarization deviation α can be expanded into a polynomial form approximately, considering the angle deviation α is a small value.

$$\cos(\alpha) \approx 1 - \frac{\alpha^2}{2} \tag{29}$$

Therefore, based on (28) and (29), α can be calculated, as shown in (30):

$$\alpha^2 \approx \frac{1}{\boldsymbol{E}_{\mathrm{m}}^2}\left[\sum_{i=1}^{3}\delta_i^2 - \left(\sum_{i=1}^{3}\frac{E_{\mathrm{m}i}}{|\boldsymbol{E}_{\mathrm{m}}|}\delta_i\right)^2\right]. \tag{30}$$

By substituting (30) into (12), we have

$$\begin{aligned} u(\alpha) &= \sqrt{\overline{\alpha^2}} \\ &\approx \sqrt{\frac{1}{\boldsymbol{E}_{\mathrm{m}}^2}\left(\overline{\sum_{i=1}^{3}\delta_i^2} - \overline{\left(\sum_{i=1}^{3}\delta_i\frac{E_{\mathrm{m}i}}{|\boldsymbol{E}_{\mathrm{m}}|}\right)^2}\right)} \\ &= \sqrt{\frac{1}{\boldsymbol{E}_{\mathrm{m}}^2}\left(\sum_{i=1}^{3}\overline{\delta_i^2}\left(1 - \frac{E_{\mathrm{m}i}^2}{\boldsymbol{E}_{\mathrm{m}}^2}\right) + 2\sum_{i=1}^{2}\sum_{j=i+1}^{3}\left(\frac{E_{\mathrm{m}i}}{|\boldsymbol{E}_{\mathrm{m}}|}\frac{E_{\mathrm{m}j}}{|\boldsymbol{E}_{\mathrm{m}}|}\overline{\delta_i\delta_j}\right)\right)} \end{aligned}, \tag{31}$$

where $u(\alpha)$ denotes the uncertainty of the polarization direction.

As mentioned above, the measured results of the components can be considered uncorrelated. Notice that δ_i and δ_j (i=1,2,3; j=1,2,3; $i\neq j$) denote the expectation of $\delta_i\delta_j$, where δ_i and δ_j are the elements of $\boldsymbol{\delta}$ shown in (4), (32) can be obtained based on (8):

$$\overline{\delta_i\delta_j} \approx \overline{\delta_i}\,\overline{\delta_j} = 0. \tag{32}$$

By substituting (7) and (32) into (31), we have:

$$\begin{aligned} u(\alpha) &\approx \frac{1}{|\boldsymbol{E}_{\mathrm{m}}|}\sqrt{\sum_{i=1}^{3}\left[\left(1-\frac{E_{\mathrm{m}i}^2}{\boldsymbol{E}_{\mathrm{m}}^2}\right)u_i^2\right]} \\ &= \frac{1}{|\boldsymbol{E}_{\mathrm{m}}|}\sqrt{u_1^2+u_2^2+u_3^2-\frac{1}{\boldsymbol{E}_{\mathrm{m}}^2}\left(E_1^2u_1^2+E_2^2u_2^2+E_3^2u_3^2\right)} \end{aligned}. \tag{33}$$

By substituting (16) into (33), we have:

$$u(\alpha) = \frac{1}{|\boldsymbol{E}_{\mathrm{m}}|}\sqrt{\sum_{i=1}^{3}u_i^2 - u^2\left(|\boldsymbol{E}_{\mathrm{m}}|\right)}. \tag{34}$$

The expression to determine the uncertainty of polarization direction is shown in (33) and (34). The uncertainty of the polarization angle can be determined using (34) directly if the amplitude uncertainty of the calculated 3D EMP has been estimated.

The range of the uncertainty of angle can be directly derived, noticed that the boundary of the amplitude uncertainty has been determined in (17) and (18), as shown in (35).

$$u(\alpha)\begin{cases} \le \dfrac{1}{|\boldsymbol{E}_{\mathrm{m}}|}\sqrt{u_1^2+u_2^2+u_3^2-\min\left(u_1^2,u_2^2,u_3^2\right)} \\ \ge \dfrac{1}{|\boldsymbol{E}_{\mathrm{m}}|}\sqrt{u_1^2+u_2^2+u_3^2-\max\left(u_1^2,u_2^2,u_3^2\right)} \end{cases} \tag{35}$$

Suppose $u_1\ge u_2\ge u_3$, the upper and lower boundaries of the polarization angle uncertainty can be determined, as shown in (36).

$$\frac{1}{|\boldsymbol{E}_{\mathrm{m}}|}\sqrt{u_2^2+u_3^2} \le u(\alpha) \le \frac{1}{|\boldsymbol{E}_{\mathrm{m}}|}\sqrt{u_1^2+u_2^2} \tag{36}$$

The upper and lower boundary can be derived based on (35), as shown in (37) and (38), to make it easier to estimate the uncertainty.

$$u(\alpha) \le \frac{\sqrt{2}}{|\boldsymbol{E}_{\mathrm{m}}|}\max\left(u_1,u_2,u_3\right) \tag{37}$$

$$u(\alpha) \ge \frac{\sqrt{2}}{|\boldsymbol{E}_{\mathrm{m}}|}\min\left(u_1,u_2,u_3\right) \tag{38}$$

Due to the detector's typical performance being identical, the three components' uncertainties will typically not vary significantly in engineering applications. As a result, there is typically

little variation between the top and lower ranges of the estimated uncertainty results. Based on (21) and the derivation of the upper and lower bounds shown in (36), we have:

$$\left|\boldsymbol{E}_{\mathrm{m}}\right|\left(\sqrt{u_1^2+u_2^2}-\sqrt{u_2^2+u_3^2}\right)=\frac{1}{\left|\boldsymbol{E}_{\mathrm{m}}\right|}\frac{u_1^2-u_3^2}{\sqrt{u_2^2+u_3^2}+\sqrt{u_1^2+u_2^2}}\le\frac{1}{\left|\boldsymbol{E}_{\mathrm{m}}\right|}\frac{u_1^2-u_3^2}{u_3+u_1}=\frac{1}{\left|\boldsymbol{E}_{\mathrm{m}}\right|}\left(u_1-u_3\right) \quad (39)$$

Therefore, the difference between the upper and lower bounds of this method can be controlled within 3%.

This section analyzed the uncertainty propagation in the 3D EMP calculation results, which can be used to evaluate the uncertainty of the amplitude and polarization angle of the 3D EMP. Before obtaining the measurement results of the three components, a rough estimate based on (19) and (36) can be made on the assumption that the measurement uncertainty evaluation results of the three components are known, and the upper and lower limits of the evaluation results can be evaluated based on (19) and (36). This is critical for mastering total vector uncertainty prior to component measurement in order to guide the measurement process. After obtaining the measurement results for three components, the component value can be replaced by the actual measurement results using (16) and (33) to calculate a relatively accurate uncertainty. There is no requirement in the extrapolation process that the uncertainty of each component conform to a certain distribution, but the assumption is made that the measurement results of each component are uncorrelated values, which may limit the evaluation of uncertainty based on the measurement results of certain detectors.

In general, the measurement is completed in a short period of time, at which time the measurement system's state and measurement settings can be regarded as the same, and the overall process's uncertainty can be viewed as the same. Indeed, due to the overlap of the measured signal and noise, the uncertainty generated by the system noise plays an important role when the amplitude (signal-to-noise ratio) is sufficiently low. The measurement amplitude will have an impact on the accuracy of each component measurement, and for pulse signal measurements in particular, the noise issue will be more pronounced at the start and end of the signal. However, we typically pay attention to the signal above half amplitude, particularly where peak-time attention is greatest. In this situation, the output signal-to-noise ratio is typically adequate, and the impact of noise relative to the overall measurement uncertainty can be disregarded. The uncertainty can be considered a time-independent value. In a strict sense, each component's measurement uncertainty counts as a time-dependent parameter. However, even if uncertainty is a time-related parameter, the conclusion of this article is equally applicable to 3D EMP uncertainty estimates, and the estimated results are time-relevant parameters as well. The simulated results apply to both the electric field (*E*) and magnetic field (*H*).

4. MCM simulation

The MCM [8] is used to simulate the uncertainty propagation in the calculation of magnitude and polarization direction. Since the purpose of the MCM simulation is to verify the uncertainty propagation in the 3D EMP calculation process deduced in Section III, this section mainly compares the results of the data in several conditions and does not cover the entire range of parameters. The simulated results apply to both the electric field (*E*) and magnetic field (*H*).

4.1. The simulation model

In the MCM simulation model, a spherical coordinate and a rectangular coordinate are established to describe the magnitude under measurement respectively. In the spherical

coordinate, the process is described by the magnitude $|\boldsymbol{E}|$ and polarization parameters θ and φ; in the rectangular coordinate, the process is described by the three orthogonal components E_1, E_2, and E_3. The definition of the two groups of parameters ($|\boldsymbol{E}|$, θ, φ) and (E_1, E_2, E_3) are shown in Fig. 1.

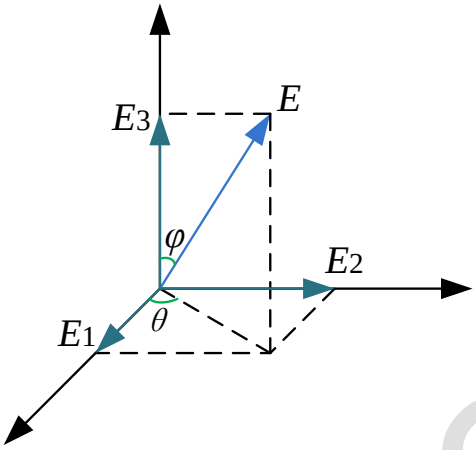

Fig.1. The spherical coordinate and the rectangular coordinate

To simplify the simulation, the magnitude of the process under measurement is normalized to 1. (40) shows the calculation formula for the three components.

$$\begin{cases} E_1 = \sin\varphi\cos\theta \\ E_2 = \sin\varphi\sin\theta \\ E_3 = \cos\varphi \end{cases} \tag{40}$$

where θ ranges from 0 to 2π, and φ ranges from 0 to π.

The measured results of components are represented by the sum of E_i (i=1,2,3) and the measuring errors δ_i (i=1,2,3) based on (40). The measuring errors are obtained by multiplying the uncertainty u_i (i=1,2,3) with the random numbers generated by the computer. This method can ensure that the statistical uncertainty of the components in the simulation is equal to the measuring uncertainty u_i (i=1,2,3).

Therefore, knowing the parameters θ, φ, u_1, u_2, and u_3, all the measured components can be obtained.

$$\begin{cases} E_{\mathrm{m1}} = \sin\varphi\cos\theta + u_1\cdot\mathrm{rand}(0,1) \\ E_{\mathrm{m2}} = \sin\varphi\sin\theta + u_2\cdot\mathrm{rand}(0,1) \\ E_{\mathrm{m3}} = \cos\varphi + u_3\cdot\mathrm{rand}(0,1) \end{cases} \tag{41}$$

where rand(0,1) denotes the random values generated in the simulation.

The measured magnitudes are calculated by (42), and the angles of the polarization directions between the measured and the given vector are calculated by (43).

$$E_{\mathrm{m}} = \sqrt{E_{\mathrm{m1}}^2 + E_{\mathrm{m2}}^2 + E_{\mathrm{m3}}^2} \tag{42}$$

$$\alpha = \arccos\left[\frac{\sum_{i=1}^{3} E_i \cdot E_{\mathrm{m}i}}{\sqrt{\sum_{i=1}^{3} E_i^2} \cdot \sqrt{\sum_{i=1}^{3} E_{\mathrm{m}i}^2}}\right] \tag{43}$$

In the MCM simulation, there are 5 variable parameters in the simulation: θ, φ, u_1, u_2, u_3. As it is difficult to completely cover all cases, some variables are fixed, and some typical values are selected to verify the estimation. Firstly, the values of θ and φ are set as $\pi/4$ while u_1, u_2 and u_3 change from 0 to 0.2. Then, u_1, u_2 and u_3 are set to 0.02 while θ and φ change to cover all the polarization directions. The reason for setting the parameters that determine the polarization angle θ and φ to $\pi/4$ is to take the intermediate value of the angle between the three components of the distance to ensure that the simulation does not degenerate into a two-dimensional or even one-dimensional situation. And the reason for setting a fixed measurement uncertainty of 0.02 is that 2% represents a typical uncertainty value for a high-quality sensor considering the engineering application.

The times of repetition are 10^6 in the MCM calculation in order to provide a coverage interval of 95% [22]. The simulated uncertainties are obtained by the RMS calculation of statistical magnitude calculated by (42) and angles calculated by (43).

4.2. Comparison of 2 different distributions

The distributions of factors that contribute to uncertainty are not necessary for the derivation of uncertainty. However, the majority of causes of uncertainty (roughly) follow a uniform or normal distribution in the evaluation of measurement uncertainty. As a consequence, the simulation primarily compares the simulation's results in the context of two different conditions, namely, uniform distribution and normal distribution.

The polarization direction is fixed first by setting θ and φ as $\pi/4$. Based on (40), E_1, E_2 and E_3 are set as 1/2, 1/2 and 1/sqrt(2) respectively. The magnitude and polarization direction uncertainties obtained by MCM, where the components follow a uniform distribution and a normal distribution, respectively, are shown in Fig. 2 and Fig. 3. The three components' measurement uncertainties vary from 0 to 0.2 in this simulation. The green points in Fig. 2 and Fig. 3 denote the simulated results based on the uniform distribution data of the three components, and the red points in Fig. 2 and Fig. 3 denote the simulated results based on the normal distribution data of the three components.

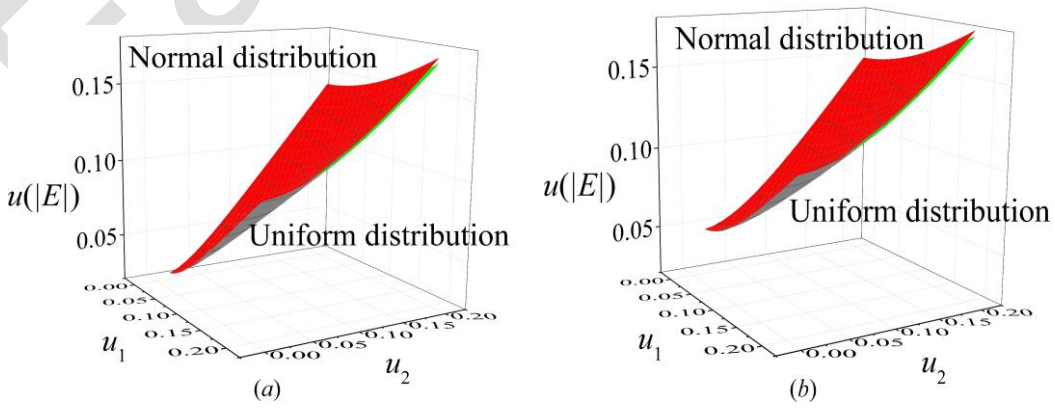

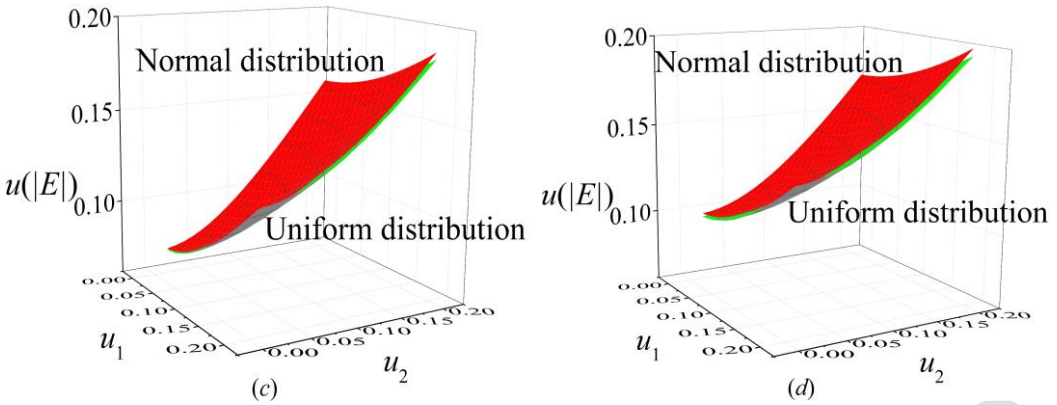

Fig. 2. Comparison of the uncertainties of the magnitude with the unform distribution and the normal distribution (θ=φ=π/4): (a) u_3=0.05; (b) u_3=0.1; (c) u_3=0.15; (d) u_3=0.2.

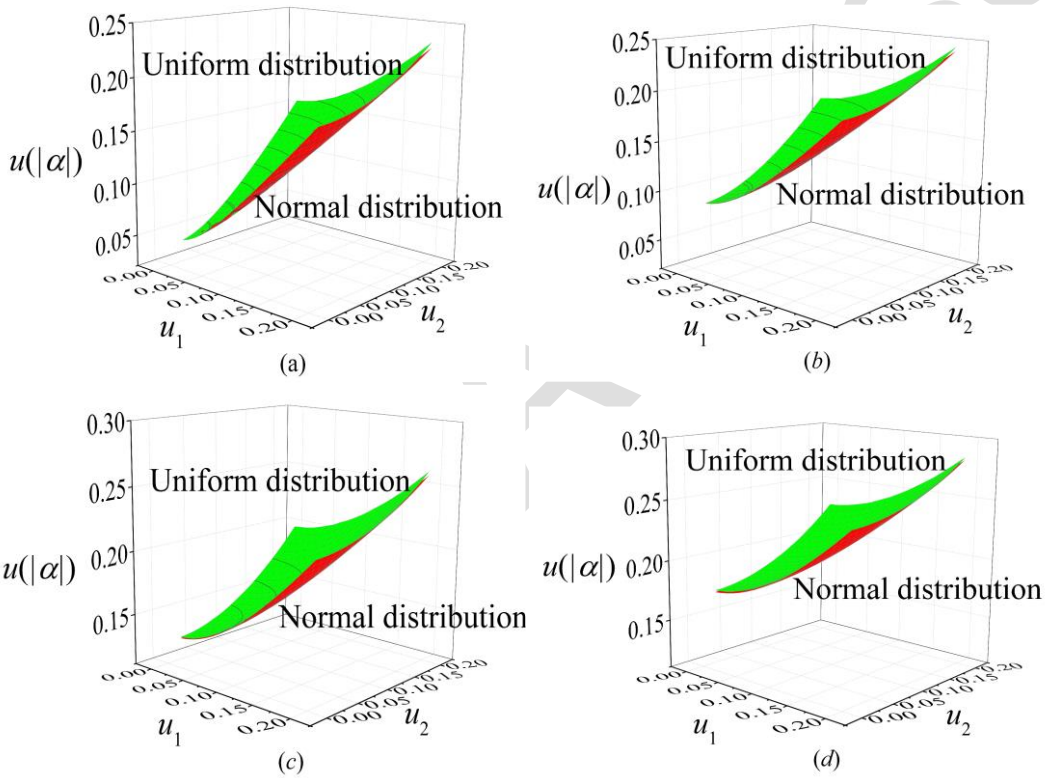

Fig. 3. Comparison of the uncertainties of the polarization direction with the unform distribution and the normal distribution (θ=φ=π/4): (a) u_3=0.05; (b) u_3=0.1; (c) u_3=0.15; (d) u_3=0.2.

The maximum (relative) differences of the uncertainties between the 2 distributions in Fig. 2(a), Fig. 2(b), Fig. 2(c), Fig. 2(d), Fig. 3(a), Fig. 3(b), Fig. 3(c) and Fig. 3(d) are 0.0035 (2.3%), 0.0033 (2.2%), 0.0035 (2.1%), 0.0043 (2.3%), 0.0082 (5.6%), 0.0073 (4.4%), 0.0059 (3.1%) and 0.0053 (2.4%), respectively, where the relative differences denote the ratio of the differences of the 2 uncertainties and the uncertainties of uniform distribution at different u_1, u_2 and u_3. The results of the MCM simulation, which were based on data from two different distributions, can be seen to be in good agreement with one another at various levels of magnitude and polarization uncertainty.

Moreover, the uncertainties of the three components are set to a fixed value of 0.02. The angle parameters θ and φ range from 0 to 2π and 0 to π respectively, which can cover all the polarization direction. In the simulation, a θ value is taken for each interval of π/25 and a φ value for each interval of π/50. A total of 2500 sets of data are numbered for different groups

of values of (θ, φ). Each number represents a fixed polarization angle according to the 2500 groups of values (θ, φ), and each group of values corresponds to an amplitude uncertainty and an angular uncertainty. Fig. 4(a) and Fig. 4(b) show the uncertainties of the magnitude and polarization directions obtained by MCM simulation based on the data of the three components with normal distribution and uniform distribution respectively. The results obtained by different distributions can be seen to be in good agreement with each other.

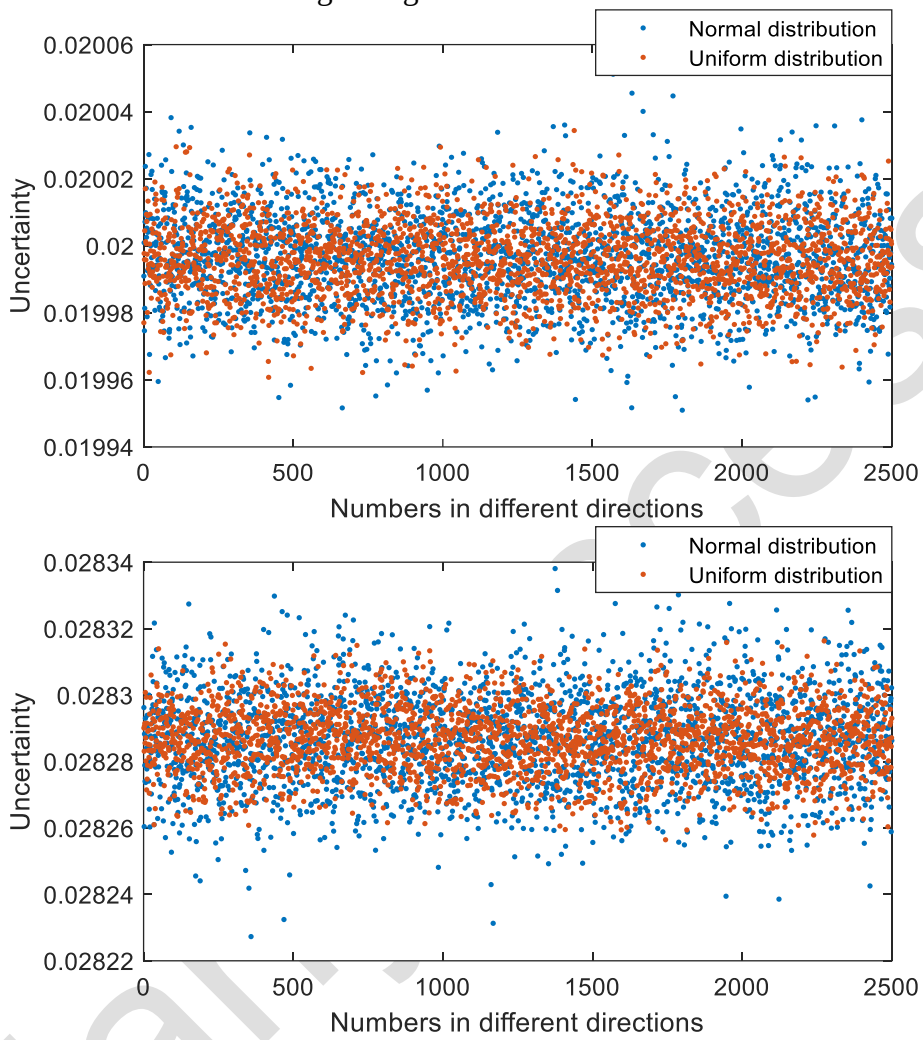

Fig. 4. Uncertainties obtained by MCM method (u_1= u_2= u_3=0.2): (a) uncertainty of the magnitude; (b) uncertainty of the polarization direction.

Although the simulation does not cover all situations and all distribution types, the results show that the uncertainty obtained under the two distributions is close to each other. There are no requirements for what distribution the uncertainty of the component should follow in the uncertainty derivation in Section III, which is also consistent with the simulation result.

4.3. Verification of the estimation formulas

Considering the most common normal distribution model, in which all components in the simulation follow a normal distribution and different components are not correlated, noticed that different distributions have no impact on simulation results. The simulated results are used to verify the estimation formulas obtained by the GUM method. The simulated results apply to both the electric field (E) and magnetic field (H).

The polarization direction is first fixed by setting θ and φ as $\pi/4$. Based on (40), E_1, E_2 and E_3 are set as 1/2, 1/2 and 1/sqrt(2) respectively. Fig. 5 and Fig. 6 show the uncertainties in magnitude and polarization direction obtained by MCM simulation and GUM estimation. The measurement uncertainties of the three components range from 0 to 0.2. The green points in Fig. 5 and Fig. 6 denote the estimated results calculated by (16) and (33) respectively, and the red points in Fig. 5 and Fig. 6 denote the results obtained by the MCM method. The maximum (relative) differences of the uncertainties between the two methods in Fig. 5(a), Fig. 5(b), Fig. 5(c), Fig. 5(d), Fig. 6(a), Fig. 6(b), Fig. 6(c) and Fig. 6(d) are 0.0026 (2.4%), 0.0034 (2.2%), 0.0036 (2.1%), 0.0044 (2.4%), 0.0083 (5.3%), 0.007 (4.0%), 0.0059 (3.0%) and 0.0053 (2.3%) respectively, where the relative differences denote the ratio of the differences of the 2 uncertainties and the uncertainties of the GUM method at different u_1, u_2 and u_3. It can be seen that the results obtained by the GUM method are in good agreement with those obtained by MCM simulation at different uncertainty values of magnitude and polarization direction.

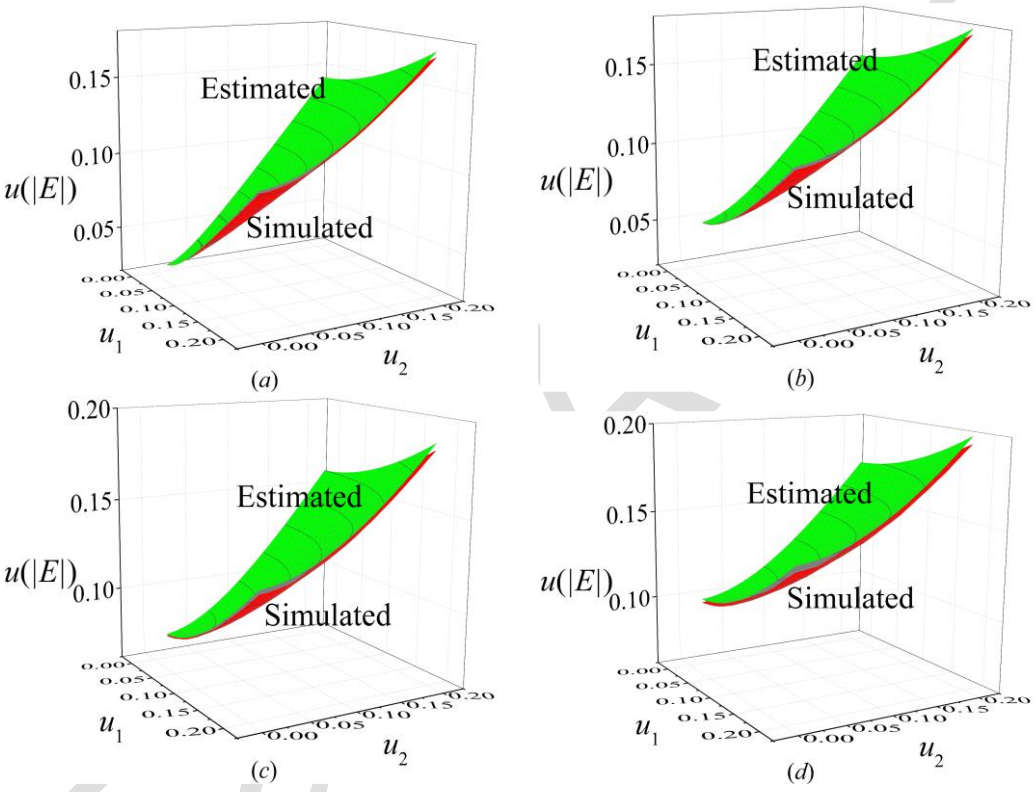

Fig. 5. Comparison of the uncertainties of the magnitude obtained by the GUM method and the MCM method (θ=φ=π/4): (a) u_3=0.05; (b) u_3=0.1; (c) u_3=0.15; (d) u_3=0.2.

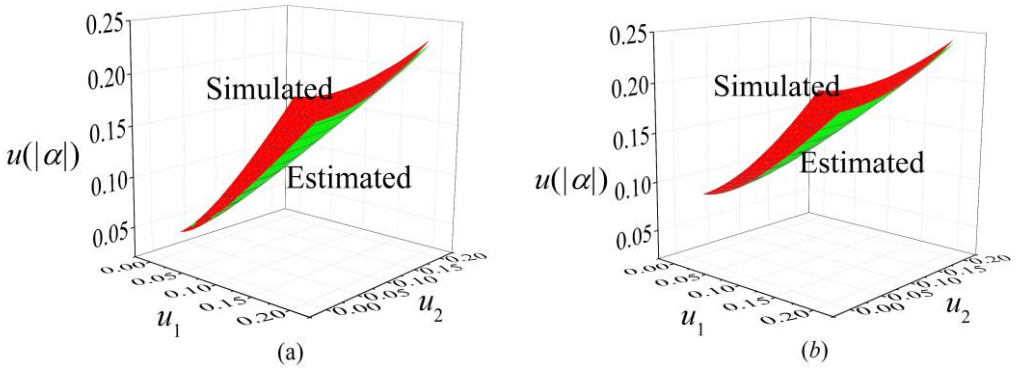

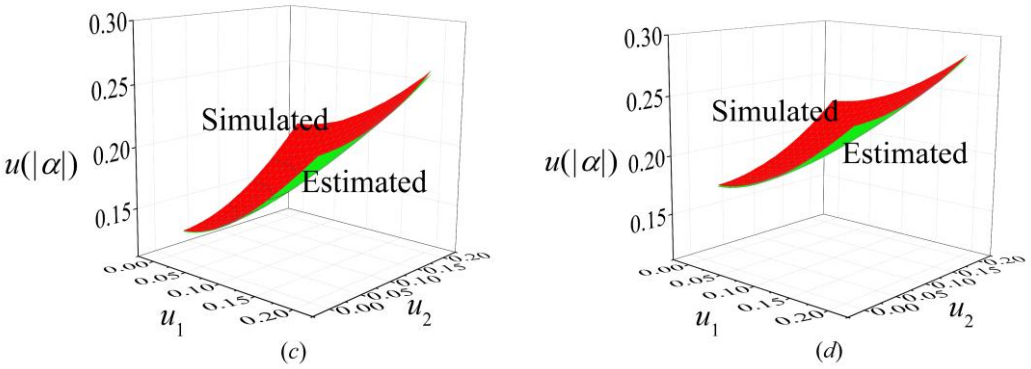

Fig. 6. Comparison of the uncertainties of the polarization direction obtained by the GUM method and the MCM method (θ=φ=π/4): (a) u_3=0.05; (b) u_3=0.1; (c) u_3=0.15; (d) u_3=0.2.

The uncertainties at different polarizations by adjusting parameters θ and φ by setting fixed uncertainties for the three components have been simulated, as shown in Fig.4. The angles range from 0 to 2π and 0 to π respectively, which can cover all the polarization directions. As the uncertainties of all the directions are the same, the calculated uncertainties of the magnitude and polarizations of the total vector are 0.02 and 0.0282 respectively. The results shown in Fig.4 obtained by the MCM method are in good agreement with the calculated results.

The uncertainty obtained by the GUM method in Section III is verified by the MCM simulation based on simulation and comparison. The calculations are straightforward and simple, which can provide a guidance in engineering applications.

5. Conclusions

In this paper, the uncertainty propagation in the calculation of 3D EMP measurement is studied, including the uncertainty of magnitude and polarization angle calculation. The results show that the uncertainty of magnitude is no more than the maximum of the uncertainty of the three components, and the uncertainty of angle is no more than sqrt(2) times of the maximum uncertainty of the three components divided by the magnitude of the measured magnitude. The conclusion can be useful for the uncertainty evaluation of 3D process measurement. All the relationships and conclusions arising from them given in the article concern the determination of the measurement uncertainty of both the electrical component (*E*) and the magnetic component (*H*) of the electromagnetic field strength. The conclusions obtained in this paper are based on the non-correlation hypothesis of the three components. It will be limited to the application of the correlation condition of the three components, which needs to be studied further.

References

[1] Shi, L., Guo, Y., Guo, J. D., & Gao, C. (2009, September). Design of magnetic field sensor for three dimensional LEMP measurement. *The Fifth Asia-Pacific Conference on Environmental Electromagnetics* (pp. 93-96). IEEE. https://doi.org/10.1109/CEEM.2009.5304318

[2] Suo, C., Wei, R., Zhang, W., & Li, Y. (2021). Research on the Three-Dimensional power frequency electric field measurement system. *Journal of Sensors*, 2021, 1-15. https://doi.org/10.1155/2021/8859022

[3] Kanda, M., & Ries, F. X. (1984). A Broad-Band Isotropic Real-Time Electric-Field Sensor (BIRES) Using Resistively Loaded Dipoles. *IEEE Transactions on Electromagnetic Compatibility, EMC-23*(3), 122-132. https://doi.org/10.1109/TEMC.1981.303931

[4] Ling, B., Wang, Y., Peng, C., Li, B., Chu, Z., Li, B., & Xia, S. (2017). Single-chip 3D electric field microsensor. Frontiers of Mechanical Engineering, *12*(4), 581-590. https://doi.org/10.1007/s11465-017-0454-x

[5] Li, W., Chen, F., & Zhang, J. (2013) An integrated optical 3D electric field sensing system based on time-division multiplexing. *Optoelectronics Letters*, *9*(4). https://doi.org/10.1007/s11801-013-3043-1

[6] Zhang, J. , Chen, F. , Sun, B. , Chen, K. , & Li, C. (2014). 3d integrated optical e-field sensor for lightning electromagnetic impulse measurement. *IEEE Photonics Technology Letters*, *26*(23), 2353-2356. https://doi.org/10.1109/LPT.2014.2355209

[7] Joint Committee for Guides in Metrology. (2008). *Evaluation of measurement data – Guide to the expression of uncertainty in measurement* (JCGM 100:2008). http://www.bipm.org/utils/common/documents/jcgm/JCGM_100_2008_E.pdf

[8] Joint Committee for Guides in Metrology. (2008). *Evaluation of measurement data – Supplement 1 to the "Guide to the expression of uncertainty in measurement" – Propagation of distributions using a Monte Carlo method* (JCGM 101:2008). https://www.bipm.org/documents/20126/2071204/JCGM_101_2008_E.pdf

[9] Coral, R., Flesch, C. A., Penz, C. A., Roisenberg, M., & Pacheco, A. L. (2016). A monte carlo-based method for assessing the measurement uncertainty in the training and use of artificial neural networks. *Metrology and Measurement Systems*, *23*(2), 281-294. https://doi.org/10.1515/mms-2016-0015

[10] Näykki, T., Virtanen, A., Kaukonen, L., Magnusson, B., Väisänen, T., & Leito, I. (2015). Application of the Nordtest method for "real-time" uncertainty estimation of on-line field measurement. *Environmental Monitoring and Assessment*, *187*(10). https://doi.org/10.1007/s10661-015-4856-0

[11] Mariscotti, A. (2007). Measurement procedures and uncertainty evaluation for electromagnetic radiated emissions from large-power electrical machinery. *IEEE Transactions on Instrumentation & Measurement, 56*(6), 2452-2463. https://doi.org/10.1109/TIM.2007.908351

[12] Meyer, V. R. (2007). Measurement uncertainty. *Journal of Chromatography A, 1158*(1-2), 15-24. https://doi.org/10.1016/j.chroma.2007.02.082

[13] Harťanský, R., Smieško, V., & Maršálka, L. (2013). Numerical analysis of isotropy electromagnetic sensor measurement error. *Measurement Science Review*, *13*(6), 311-314. https://doi.org/10.2478/msr-2013-0046

[14] Jakubowski, J. (2020). A study on the calibration of an HPM meter based on a D-dot sensor and logarithmic RF power detector. *Metrology and Measurement Systems*, *27*(4), 673-685. https://doi.org/10.24425/mms.2020.134846

[15] Kong, X., & Xie, Y. Z. (2015, November). Measurement uncertainty analysis of the electro-optical E-field measurement system. *2015 7th Asia-Pacific Conference on Environmental Electromagnetics (CEEM)* (pp. 296-298). *IEEE*. 296-298. https://doi.org/10.1109/CEEM.2015.7368689

[16] Kanda, M. (1994). Standard antennas for electromagnetic interference measurements and methods to calibrate them. *IEEE Transactions on Electromagnetic Compatibility*, *36*(4), 261-273. https://doi.org/10.1109/15.328855

[17] Liu, X., Meng, D.-L., Huang, P., et. al. (2021). The Loop Antenna Calibration System Using the TEM Method and the Uncertainty Estimation for the Measurement Results. *Jiliang Xuebao/Acta Metrologica Sinica*, *42*(8) 1061-1067. https://doi.org/10.3969/j.issn.1000-1158.2021.08.13

[18] Shi, Y., Nie, X., Zhu, Z., Wang, W., & Wang, J. (2019). Study of the fitting method in the sensitivity calibration of a hemp measuring system. *IEEE Transactions on Electromagnetic Compatibility*, *62*(4), 1-7. https://doi.org/10.1109/TEMC.2019.2929117

[19] Majerek, D., Widomski, M., Garbacz, M., & Suchorab, Z. (2018, July). Estimation of the measurement uncertainty of humidity using a TDR probe. In *AIP Conference Proceedings* (Vol. 1988, No. 1). AIP Publishing. https://doi.org/10.1063/1.5047621

[20] Peng, H., & Jiang, X., (2009). Evaluation and management procedure of measurement uncertainty in new generation geometrical product specification (GPS). *Measurement, 42*(5), 653–660. https://doi.org/10.1016/j.measurement.2008.10.009

[21] Yapeng, F., Zheng, S., Yueqi, H., Yun, Z., & Zheng, K. (2021, December). Research on a New Flat Plate Lightning Three-dimensional Electric Field Sensor. In *2021 13th International Symposium on Antennas, Propagation and EM Theory (ISAPE)* (pp. 1-3). IEEE. https://doi.org/10.1109/ISAPE54070.2021.9752858

[22] Bing, L. I., Chunrong, P., Biyun, L., Fengjie, Z., Bo, C., & Shanhong, X. (2017). The decoupling calibration method based on genetic algorithm of three-dimensional electric field sensor. *Dianzi Yu Xinxi Xuebao/Journal of Electronics and Information Technology*, *39*(9), 2252-2258. https://doi.org/10.11999/JEIT161277 (in Chinese)

[23] Solaguren-Beascoa Fernández, M., Alegre Calderon, J. M., & Bravo Díez, P. M. (2009). Implementation in MATLAB of the adaptive Monte Carlo method for the evaluation of measurement uncertainties. *Accreditation and Quality Assurance*, *14*(2), 95-106. https://doi.org/10.1007/s00769-008-0475-6

Yuewu Shi was born in Mianyang, China, in 1990. He received the B.S. degree from Nanjing University, Nanjing, China, in 2012, and the M.S. degree from the Northwest Institute of Nuclear Technology (NINT), Xi'an, China, in 2015. Since 2012, he has been at NINT. He is currently an Assistant Researcher with NINT and his research interests include EMP test, effect and measurement.

Wei Wang was born in Zhangye, China, in 1984. He received the B.S. degree from Wuhan University, Wuhan, China, in 2007, and the M.S. degree from Northwest Institute of Nuclear Technology (NINT), Xi'an, China, in 2010. Since 2007, he has been at NINT. He is currently an Associate Researcher with NINT and his research interests include EMP test and measurement.

Xin Nie was born in Jilin, China, in 1977. He received the B.S. degree from Jilin University, Jilin, China, in 2000, and the M.S. degree from the Northwest Institute of Nuclear Technology (NINT), Xi'an, China, in 2006. Since 2000, he has been at NINT. He is currently a Researcher with NINT. His research interests include EMP effect and test.

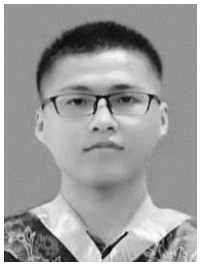

Jianguo Miao was born in Handan, China, in 1995. He received the B.S. degree and the M.S. degree from National University of Defense Technology, Changsha, China, in 2017 and 2019 respectively. Since 2019, he has been at the Northwest Institute of Nuclear Technology (NINT), Xi'an. He is currently an Assistant Researcher with NINT and his research interests include EMP test and measurement.

Wei Chen received the Ph.D. degree in nuclear science and technology from Xi'an Jiaotong University, Xi'an, China, in 1998. He is the Vice President and Secretary of the Chinese Nuclear Society Radiation Physics Branch. He has almost 200 publications in many kinds of scientific journals, including IEEE TRANSACTIONS ON NUCLEAR SCIENCE and Nuclear Instruments and Methods in Physics Research. He majors in radiation effects.